Advances in Nano Research, *Vol. 5, No. 4 (2017) 281-301*
DOI: https://doi.org/10.12989/anr.2017.5.4.281

Investigating vibration behavior of smart imperfect functionally graded beam subjected to magnetic-electric fields based on refined shear deformation theory

Farzad Ebrahimi * and Ali Jafari

Department of Mechanical Engineering, Faculty of Engineering,
Imam Khomeini International University, Qazvin, Iran

(*Received November 29, 2016, Revised February 20, 2017, Accepted March 30, 2017*)

Abstract. In this disquisition, an exact solution method is developed for analyzing the vibration characteristics of magneto-electro-elastic functionally graded (MEE-FG) beams by considering porosity distribution and various boundary conditions via a four-variable shear deformation refined beam theory for the first time. Magneto-electro-elastic properties of porous FG beam are supposed to vary through the thickness direction and are modeled via modified power-law rule which is formulated using the concept of even and uneven porosity distributions. Porosities possibly occurring inside functionally graded materials (FGMs) during fabrication because of technical problem that lead to creation micro-voids in FG materials. So, it is necessary to consider the effect of porosities on the vibration behavior of MEE-FG beam in the present study. The governing differential equations and related boundary conditions of porous MEE-FG beam subjected to physical field are derived by Hamilton's principle based on a four-variable tangential-exponential refined theory which avoids the use of shear correction factor. An analytical solution procedure is used to achieve the natural frequencies of porous-FG beam supposed to magneto-electrical field which satisfies various boundary conditions. A parametric study is led to carry out the effects of material graduation exponent, porosity parameter, external magnetic potential, external electric voltage, slenderness ratio and various boundary conditions on dimensionless frequencies of porous MEE-FG beam. It is concluded that these parameters play noticeable roles on the vibration behavior of MEE-FG beam with porosities. Presented numerical results can be applied as benchmarks for future design of MEE-FG structures with porosity phases.

Keywords: magneto-electro-elastic FG material; porous materials; analytical solution; free vibration; refined beam theory

1. Introduction

Technology development in field of making materials with functional properties introduce Functionally graded materials (FGMs) as a new class of smart composite structures which have led many researchers to analyze the mechanical specifications of these materials with engineering structure like beam, plate and shell. Due to high strength and high temperature resistance of FGMs, they are increasingly utilized in the mechanical, civil, nuclear reactors, aerospace engineering and etc. as structural components (Ebrahimi and Rastgoo 2009, Ebrahimi *et al*. 2009, Ebrahimi and

*Corresponding author, Ph.D., E-mail: febrahimy@eng.ikiu.ac.ir

 ISSN: 2287-237X (Print), 2287-2388 (Online)

Sepiani 2010). Numerous studies have been conducted for investigation the mechanical responses of FG structures (Ebrahimi and Rastgoo 2011, Ebrahimi *et al*. 2010, Ebrahimi 2013, Ebrahimi and Jafari 2016a, b, Akbas 2015). Due to immense applications of smart materials in contemporary technology, intelligent structures made of magneto electro elastic materials (MEEMs) are nowadays widely utilized in engineering fields. In 1990s, in two-phase composites of piezoelectric and piezo-magnetic materials, a strong magneto-electrical coupling effect was discovered which has potential practical application in many fields (Harshe *et al*. 1993) and reported that this coupling effect cannot be found in a single-phase material.

Furthermore, MEEMs shows some fascinating properties such as the piezo-electric, piezo-magnetic and magneto-electric influences in which the elastic deformations may be produced directly by mechanical loading or indirectly by an application of electric or magnetic field. Due to their superior properties, these materials may exhibit particular specifications that make them acting as mechanical sensors, controller and actuators for converting energy (Zhang *et al*. 2014). Owing to these advantages, MEE have received wide applications in modern industries such as aircraft structures, vibration control of civil infrastructure; stress monitoring and nondestructive testing (Song *et al*. 2006). Hitherto, many researchers attracted to discover mechanical response of structures made of MEEMs. Among them, Pan (2001) provided three dimensional exact solutions for simply-supported anisotropic MEE multilayered rectangular plate subjected to surface and internal loads. By analytical solution method, Jiang and Ding (2004) analyzed vibration behavior of magneto-electro-elastic beams. Vibration responses of non-homogenous isotropic MEE plates is reported by Chen *et al*. (2005). Kumaravel *et al*. (2007) researched thermal stability and vibrational behavior of layered and multiphase magneto-electro-elastic beams. By implementation of finite element method, transient dynamic response of multiphase magneto-electro-elastic cantilever beam is presented by Daga *et al*. (2009). Razavi and Shooshtari (2015) presented nonlinear vibration investigation of a magneto-electro-elastic laminated plate based on first order shear deformation theory with SSSS boundary condition, whereas Maxwell equations for electrostatics and magneto-statics are used to model the electric and magnetic behavior. Most recently, based on three-dimensional elasticity theory and employing the state space approach, Xin and Hu (2015) presented semi-analytical evaluation of free vibration of arbitrary layered magneto-electro-elastic beams.

For more efficient and expand applications of magneto electro elastic structures, they were recently synthesized by using FGMs. Actually, functionally graded model enables the MEEMs to have the best properties. Recent investigation about of MEEMs discusses mechanical response of structural elements made of functional graded MEEMs. Pan and Han (2005) provided exact solution for analysis of the rectangular plates composed of functionally graded, anisotropic, and linear magneto-electro-elastic materials. Furthermore, the plane stress problem of a MEE-FG beam were inspected by Huang *et al*. (2007) using an analytical method. In another survey, Wu and Tsai (2007) examined static behavior of a doubly curved MEE-FG shell employing an asymptotic approach. Based on higher order shear deformation theory, a theoretical study on buckling and vibration behavior of FG magneto electro thermo elastic circular cylindrical shell was carried out by Lang and Xuewu (2013). Kattimani and Ray (2015) researched large amplitude vibration responses of MEE-FG plates. Static behavior of a circular MEE-FG plate under different boundary conditions is demonstrated by Sladek *et al*. (2015) by using a meshless local Petrov–Galerkin method.

With the rapid development in technology of structural elements, structures with graded porosity can be introduced as one of the latest development in FGMs. The structures consider

pores into microstructures by taking the local density into account. Researches focus on development in preparation methods of FGMs such as powder metallurgy, vapor deposition, self-propagation, centrifugal casting, and magnetic separation. These methods have their own ineffectiveness such as complexity of the technique and high costs. An efficient way to manufacture FGMs is sintering process in which due to difference in solidification of the material constituents, porosities or micro-voids through material can create (Zhu *et al*. 2001). An investigation has been carried out on porosities existing in FGMs fabricated by a multi-step sequential infiltration technique (Wattanasakulpong *et al*. 2012). According to this information, for building more secure and accurate structures it is important to consider the porosity impact on designing FGM structures. Porous FG structures have many interesting combinations of mechanical properties, such as high stiffness in conjunction with very law specific weight (Rezaei and Saidi 2016). Since porous FG structures have reached remarkable attention by many engineers, recent paper in field of FG structures consider mechanical response of structural ingredients made of functional graded materials with porosities. Wattanasakulpong and Ungbhakorn (2014) examined the linear and non-linear vibration of porous FGM beams with elastically restrained ends. Ebrahimi and Mokhtari (2014) provided differential transform method to examine vibration behavior of rotating Timoshenko porous FG beams. They reported that porosity volume fraction has a key role on the vibrational response of the FG beams. In order to predict flexural vibration of porous FGM Timoshenko beams, Wattanasakulpong and Chaikittiratana (2015) employed Chebyshev collocation method. Ebrahimi and Zia (2015) utilized the Galerkin and multiple scales methods to study nonlinear vibration of porous FGM beams. Static analysis of porous FG plate is examined by Benferhat *et al.* (2016). Ebrahimi *et al.* (2016a) presented thermo-mechanical vibration response of temperature-dependent porous FG beams exposed to various temperature risings based on classic beam theory (CBT) which disregards the influence of shear deformation. In other words, CBT is unable to model thick beams and higher modes of vibration. Hereupon, first order shear deformation theory (FSDT) is suggested to overcome the defects of CPT with supposition a shear correction factor in the thickness direction of beam (Ebrahimi and Barati 2016c). As respects FSDT isn't able to evaluate the zero-shear stress on the top and bottom surfaces of the beam, there appeared a need to develop new theory. In order to bypass these defects, higher order shear deformation theory (HSDT) was introduced. This theory predicts transverse shear stresses without need of any shear correction factors. Many papers are published with the framework of HSDT to investigate mechanical response of FG structures (Ebrahimi and Barati 2016c). Moreover, Yahia *et al*. (2015) study the porosity effect on the wave propagation of FG plates by using various higher-order shear deformation theories. Recently, Mechab *et al.* (2016) developed nonlocal two-variable refined plate theory for free vibration of FG porous nanoplates resting on elastic foundations. It is worth mentioning although various inclusion-related study about of vibration of porous FG beam have been perused in recent years, no published work considering magneto-electrical field on vibration response of smart FG beams with different porosity distributions and boundary conditions based on four-variable refined shear deformation theory. Analysis of nano-structure's mechanical behaviors is one of recent interesting research topics (Ebrahimi and Barati 2016a-i, Ebrahimi and Barati 2017). For instance, thermal buckling, wave propagation and free vibration analysis of FG nanobeams subjected to temperature distribution have been exactly investigated by Ebrahimi and Salari (2016, 2015a-d) and Ebrahimi and Barati (2016j, k) and Ebrahimi *et al.* (2015a, b). Ebrahimi and Barati (2016l-n) and Ebrahimi and Salari (2016b-d) investigated buckling behavior of smart piezoelectrically actuated higher-order size-dependent graded nanoscale beams and plates in thermal environment. The thermo-

mechanical nonlinear vibration behaviors of size-dependent nanoplates are investigated by Ebrahimi and Hosseini (2016b). Ebrahimi and Shafiei (2016) showed the effects of existing initial shear stress in the vibration analysis of orthotropic single layered graphene sheets based on the nonlocal elasticity. The mentioned positive points are interesting enough for the authors to employ FGMs in researches dealing with the mechanical behavior of structures (Ebrahimi *et al*. 2016a-e); Ebrahimi and Barati 2016o-s, Ebrahimi and Hosseini 2016b, Ebrahimi and Boreiry 2015). Thermo-electro-mechanical static and dynamic responses of circular FG plates are discussed and presented by Ebrahimi. Ebrahimi *et al*. showed the influences of thermal loading parallel with porosity effects on vibration properties of FG temperature-dependent beams.

The present research makes the first achievement to develop a four-variable refined shear deformation theory for transverse vibration of magneto-electro-porous FG beams with various boundary conditions. Refined beam theory considers a constant transverse displacement and higher-order variation of axial displacement through the depth of the beam so that there is no need for any shear correction factors. Two kinds of porosity distribution namely even and uneven through the thickness directions are considered. The modified power-law model is exploited to describe gradual variation of material properties of the porous MEE-FG beam. Applying Hamilton's principle, governing equations of higher order MEE-FG beam are obtained together based on four-variable refined shear deformation theory and they are solved applying an analytical solution method. Several numerical exercises indicate that various parameters such as magnetic potential, external electric voltage, porosity volume fraction, types of porosity distribution, material graduation index and various boundary conditions have remarkable influence on fundamental frequencies of porous MEE-FG beam.

2. Theory and formulation

2.1 Power-low functionally graded beams with porosities

Consider a magneto-electro-elastic functionally graded beam with two different porosity distribution and rectangular cross-section of length (L), width (b) and thickness (h) according to Fig. 1(a). MEE-FG beam is composed of Barium titanate ($BaTio_3$) and Cobalt Ferrite ($CoFe_2O_4$) with the material properties presented in Table 1 and exposed to a magnetic potential $\gamma(x, z, t)$ and electric potential $\Phi(x, z, t)$. The effective material properties of MEE-FG beam change continuously in the thickness direction according to modified power-law distribution. The effective material properties (P_f) of porous FGM beam by using the modified rule of mixture can be written as (Wattanasakulpong and Ungbhakorn 2014)

$$P_f = P_u(V_u - \frac{\alpha}{2}) + P_l(V_l - \frac{\alpha}{2}) \tag{1}$$

Which α defines the volume fraction of porosities, for a perfect FGM α is equal to zero, P_u and P_l are the material properties of top and bottom directions, V_u and V_l are the volume fraction of top and bottom sides, respectively, which can be linked according to

$$V_u + V_l = 1 \tag{2}$$

Then the volume fraction of upper side (V_u) is given by

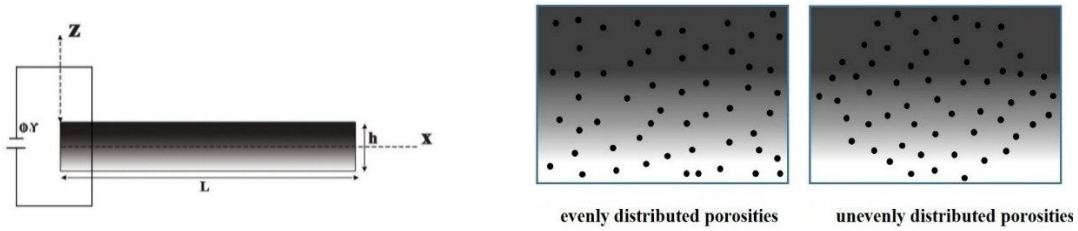

(a) (b)

Fig. 1 Geometry and cross section of porous FGM beam under magneto-electrical field

Table 1 Magneto-electro-elastic coefficients of material properties

Properties	$BaTiO_3$	$CoFe_2O_4$	Properties	$BaTiO_3$	$CoFe_2O_4$
$c_{11} = c_{22}$ (GPa)	166	286	e_{15}	11.6	0
c_{33}	162	269.5	q_{31} (N/Am)	0	580.3
$C_{13} = c_{23}$	78	170.5	q_{33}	0	699.7
c_{12}	77	173	q_{15}	0	550
c_{55}	43	45.3	s_{11} ($10^{-9}C^2m^{-2}N^{-1}$)	11.2	0.08
c_{66}	44.5	56.5	s_{13}	12.6	0.093
e_{31} (Cm^{-2})	-4.4	0	χ_{11} ($10^{-6}Ns^2C^{-2}/2$)	5	-590
e_{33}	18.6	0	χ_{33}	10	157
ρ (kgm^{-3})	5800	5300	$d_{11} = d_{22} = d_{33}$	0	0

$$V_u = \left(\frac{z}{h} + \frac{1}{2}\right)^P \tag{3}$$

Where ($p \geq 0$) is a non-negative parameter (power-law exponent or the volume fraction index) which determines the material distribution across the beam thickness.

According to Eqs. (1)- (2), the effective material properties of porous MEE-FG (I) beam with even porosities are variable across the thickness direction with the following form

$$P(z) = \left(P_u - P_l\right)\left(\frac{z}{h} + \frac{1}{2}\right)^p + P_l - \left(P_u + P_l\right)\frac{\alpha}{2} \tag{4}$$

It must be noted that, the top surface at $z = +h/2$ of porous MEE-FG beam is fully $CoFe_2O_4$, whereas the bottom surface ($z = -h/2$) is fully $BaTio_3$. Moreover, the MEE-FG (II) beam has porosity phases spreading frequently nearby the middle zone of the cross-section and the amount of porosity seems to be linearly decrease to zero at the top and bottom of the cross-section. Fig. 1(b) demonstrates cross-section areas of FGM-I and-II with porosities phases. For uneven distribution of porosities, the effective material properties are replaced by following form.

$$P(z) = \left(P_u - P_l\right)\left(\frac{z}{h} + \frac{1}{2}\right)^p + P_l - \frac{\alpha}{2}\left(P_u + P_l\right)\left(1 - \frac{2|z|}{h}\right) \tag{5}$$

2.2 Kinematic relations

Based on new tangential-exponential refined shear deformation beam theory, the displacement field at any point of the beam can be expressed as

$$u_1(x,z,t) = u(x,t) - z\frac{\partial w_b}{\partial x} - f(z)\frac{\partial w_s}{\partial x} \tag{6}$$

$$u_3(x,z,t) = w_b(x,t) + w_s(x,t) \tag{7}$$

Which u is displacement of mid-plane along x and w_b, w_s are the bending and shear components of transverse displacement of a point on the mid-plane of the beam and t is the time. $f(z)$ denotes a shape function estimating the distribution of shear stress across the beam thickness. $f(z)$ is considered to satisfy the stress-free boundary conditions on the top and bottom sides of the beam. So, it is not required to use any shear correction factor. The present theory has a function in the form Mantari *et al*. (2014)

$$f(z) = \tan\left[(\frac{\pi z}{2h})\right] r^{\sec\left[(\frac{\pi z}{2h})\right]}, \quad r = 0.03 \tag{8}$$

The electric potential and magnetic potential distributions across the thickness are approximated via a combination of a cosine and linear variation to satisfy Maxwell's equation in the quasi-static approximation as follows (Ke and Wang 2014)

$$\Phi(x,z,t) = -\cos(\xi(z))\phi(x,t) + \frac{2z}{h}V \tag{9}$$

$$\Upsilon(x,z,t) = -\cos(\xi(z))\gamma(x,t) + \frac{2z}{h}\Omega \tag{10}$$

where $\xi = \pi / h$. Also, V and Ω are the external electric voltage and magnetic potential applied to the MEE-FG beam. Nonzero strains of the four-variable beam model are expressed by

$$\varepsilon_{xx} = \frac{\partial u}{\partial x} - z\frac{\partial^2 w_b}{\partial x^2} - f\left(\frac{\partial^2 w_s}{\partial x^2}\right) \tag{11}$$

$$\gamma_{xz} = (1 - \frac{\partial f}{\partial x})\frac{\partial w_s}{\partial x} = g\frac{\partial w_s}{\partial x} \tag{12}$$

where ε_{XX}, γ_{xz} are the normal and shear strains and $g(z) = \left(1 - \frac{df}{dz}\right)$ is the shape function of the transverse shear strains. According to Eq. (9), the relation between electric field (E_x, E_y, E_z) and electric potential (Φ) can be obtained as (Wu and Tsai 2010)

$$E_x = -\Phi_{,x} = \cos(\xi(z))\frac{\partial \phi}{\partial x}, \tag{13}$$

$$E_z = -\Phi_{,z} = -\xi \sin(\xi(z))\phi - \frac{2V}{h} \tag{14}$$

Also, the relation between magnetic field (H_x, H_y, H_z) and magnetic potential (Υ) can be expressed from Eq. (10) as (Wu and Tsai 2010)

$$H_x = -\Upsilon_{,x} = \cos(\xi(z))\frac{\partial \gamma}{\partial x}, \tag{15}$$

$$H_z = -\Upsilon_{,z} = -\xi \sin(\xi(z))\gamma - \frac{2\Omega}{h} \tag{16}$$

Through extended Hamilton's principle, the equation of motion can be derived by

$$\int_{t_1}^{t_2} \delta(U - T + V)\, dt = 0 \tag{17}$$

Here U is strain energy, V is work done by external forces and T is kinetic energy. The following Euler–Lagrange equations are obtained by utilizing the virtual work principle and setting the coefficients of δu, δw_b, δw_s, $\delta\phi$ and $\phi\gamma$ to zero

$$(\delta u : 0),\ \frac{\partial N}{\partial x} = I_0 \frac{\partial^2 u}{\partial t^2} - I_1 \frac{\partial^3 w_b}{\partial t^2 \partial x} - J_1 \frac{\partial^3 w_s}{\partial t^2 \partial x} \tag{18}$$

$$\begin{aligned}(\delta w_b : 0),\ & \frac{\partial^2 M_b}{\partial x^2} - \bar{N}\frac{\partial^2 (w_s + w_b)}{\partial x^2} \\ & = I_0\left(\frac{\partial^2 w_s}{\partial t^2} + \frac{\partial^2 w_b}{\partial t^2}\right) + I_1 \frac{\partial^3 u}{\partial t^2 \partial x} - I_2 \frac{\partial^4 w_b}{\partial t^2 \partial x^2} - J_2 \frac{\partial^4 w_s}{\partial t^2 \partial x^2}\end{aligned} \tag{19}$$

$$\begin{aligned}(\delta w_s : 0),\ & \frac{\partial^2 M_x^s}{\partial x^2} + \frac{\partial Q_{xz}}{\partial x} - \bar{N}\frac{\partial^2 (w_s + w_b)}{\partial x^2} \\ & = I_0\left(\frac{\partial^2 w_s}{\partial t^2} + \frac{\partial^2 w_b}{\partial t^2}\right) - k_2 \frac{\partial^4 w_b}{\partial t^2 \partial x^2} + J_1 \frac{\partial^3 u}{\partial t^2 \partial x} - J_2 \frac{\partial^4 w_b}{\partial t^2 \partial x^2}\end{aligned} \tag{20}$$

$$(\delta\phi = 0),\ \int_{\frac{-h}{2}}^{\frac{h}{2}} \left(\cos(\xi z)\frac{\partial D_x}{\partial x} + \xi \sin(\xi z) D_z\right) dz = 0 \tag{21}$$

$$(\delta\gamma = 0),\ \int_{\frac{-h}{2}}^{\frac{h}{2}} \left(\cos(\xi z)\frac{\partial B_x}{\partial x} + \xi \sin(\xi z) B_z\right) dz = 0 \tag{22}$$

In which the variables introduced (N, M_b, M_s, Q), mass moment of inertias (I_0, I_1, I_2, J_1, J_2, K_2) are defined as

$$N = \int_A \sigma_{xx} dA, M_b = \int_A \sigma_{xx} z dA, M_s = \int_A \sigma_{xx} f dA, Q = \int_A \sigma_{xz} g dA \tag{23}$$

$$I_0 = \int_A \rho(z,T)\, dA, I_1 = \int_A \rho(z,T)\, zdA, I_2 = \int_A \rho(z,T)\, z^2 dA, J_1 = \int_A \rho(z,T)\ fdA,$$
$$J_2 = \int_A \rho(z,T)\ fzdA, K_2 = \int_A \rho(z,T)\ f^2 dA \tag{24}$$

In this study it assumed that the porous MEE-FG beam is under external electric voltage and magnetic potential. So, $\bar{N}$ is the normal forces induced by external electric voltage V (N^E) and external magnetic potential Ω (N^H), respectively and are defined as

$$\bar{N} = N^E + N^H, \qquad \{N^E, N^H\} = -\int_{-h/2}^{h/2} \{\tilde{e}_{31} V, \tilde{q}_{31}\, \Omega\} \frac{2}{h}\, dz \tag{25}$$

For a linear MEE porous FG beam exposed to magneto-electro mechanical loading, the coupled constitutive relations may be rewritten as (Wu *et al*. 2010)

$$\sigma_{ij} = C_{ijkl}\varepsilon_{kl} - e_{mij}E_m - q_{nij}H_n \tag{26}$$

$$D_i = e_{ikl}\varepsilon_{kl} + k_{im}E_m + d_{in}H_n \tag{27}$$

$$B_i = q_{ikl}\varepsilon_{kl} + d_{im}E_m + \chi_{in}H_n \tag{28}$$

which σ_{ij}, D_i, B_i denotes the components of stress, electric displacement and magnetic induction, ε_{kl}, E_m and H_n are the components of linear strain, electric field and magnetic field. Additionally, C_{ijkl}, k_{im} and χ_{in} are the components of elastic stiffness, dielectric permittivity and magnetic permittivity coefficients; Finally, e_{mij}, q_{nij}, and d_{in} are the piezoelectric, piezo-magnetic, and magneto-electric-elastic coefficients, respectively. By integrating Eq. (26)-(28) over the area of MEE porous FG beam cross-section, the following relations for the force-strain and the moment-strain and other necessary relation of the refined FG beam can be obtained

$$N = A_{11}\frac{\partial u}{\partial x} - B_{11}\frac{\partial^2 w_b}{\partial x^2} - B_{11}^S \frac{\partial^2 w_s}{\partial x^2} + A_{31}^e \varphi + A_{31}^m \gamma - N_x^E - N_x^H, \tag{29}$$

$$M_b = B_{11}\frac{\partial u}{\partial x} - D_{11}\frac{\partial^2 w_b}{\partial x^2} - D_{11}^s \frac{\partial^2 w_s}{\partial x^2} + E_{31}^e \varphi + E_{31}^m \gamma - M_{bx}^E - M_{bx}^H \tag{30}$$

$$M_s = B_{11}^S \frac{\partial u}{\partial x} - D_{11}^s \frac{\partial^2 w_b}{\partial x^2} - H_{11}^s \frac{\partial^2 w_s}{\partial x^2} + F_{31}^e \phi + F_{31}^m \gamma - M_{sx}^E - N_{sx}^H \tag{31}$$

$$Q = A_4^S \frac{\partial w_s}{\partial x} - A_{15}^e \frac{\partial \phi}{\partial x} - A_{15}^m \frac{\partial \gamma}{\partial x} \tag{32}$$

$$\int_{-\frac{h}{2}}^{\frac{h}{2}} D_x \cos(\xi z) dz = E_{15}^e \frac{\partial w_s}{\partial x} + F_{11}^e \frac{\partial \phi}{\partial x} + F_{11}^m \frac{\partial \gamma}{\partial x} \tag{33}$$

$$\int_{-\frac{h}{2}}^{\frac{h}{2}} D_z\, \xi \sin(\xi z) dz = A_{31}^e (\frac{\partial u}{\partial x}) - E_{31}^e \nabla^2 w_b - F_{31}^e \nabla^2 w_s - F_{33}^e \phi - F_{33}^m \gamma \tag{34}$$

$$\int_{-\frac{h}{2}}^{\frac{h}{2}} B_x \cos(\xi z)dz = E_{15}^m \frac{\partial w_s}{\partial x} + F_{11}^m \frac{\partial \phi}{\partial x} + X_{11}^m \frac{\partial \gamma}{\partial x} \tag{35}$$

$$\int_{-\frac{h}{2}}^{\frac{h}{2}} B_z \, \xi \sin(\xi z)dz = A_{31}^m (\frac{\partial u}{\partial x}) - E_{31}^m \nabla^2 w_b - F_{31}^m \nabla^2 w_s - F_{33}^m \phi - X_{33}^m \gamma \tag{36}$$

And the last form of Euler-Lagrange equations for MEE porous FG based on four-variable refined shear deformation beam theory in terms of displacement u, w_b, w_s, ϕ and γ can be derived as

$$A_{11} \frac{\partial^2 u}{\partial x^2} - B_{11} \frac{\partial^3 w_b}{\partial x^3} - B_{11}^s \frac{\partial^3 w_s}{\partial x^3} + A_{31}^e \frac{\partial \phi}{\partial x} + A_{31}^m \frac{\partial \gamma}{\partial x} - I_0 \frac{\partial^2 u}{\partial t^2} + I_1 \frac{\partial^3 w_b}{\partial x \partial t^2} + J_1 \frac{\partial^3 w_s}{\partial x \partial t^2} = 0 \tag{37}$$

$$\begin{aligned} &B_{11} \frac{\partial^3 u}{\partial x^3} - D_{11} \frac{\partial^4 w_b}{\partial x^4} + E_{31}^e \frac{\partial^2 \phi}{\partial x^2} - D_{11}^s \frac{\partial^4 w_s}{\partial x^4} + E_{31}^m \frac{\partial^2 \gamma}{\partial x^2} - I_0 \frac{\partial^2 (w_b + w_s)}{\partial t^2} - I_1 (\frac{\partial^3 u}{\partial x \partial t^2}) + \\ &I_2 (\frac{\partial^4 w_b}{\partial x^2 \partial t^2}) + J_2 (\frac{\partial^4 w_s}{\partial x^2 \partial t^2}) - (\bar{N}) \frac{\partial^2 (w_b + w_s)}{\partial x^2} = 0 \end{aligned} \tag{38}$$

$$\begin{aligned} &B_{11}^s \frac{\partial^3 u}{\partial x^3} - D_{11}^s \frac{\partial^4 w_b}{\partial x^4} + A_{55}^s \frac{\partial^2 w_s}{\partial x^2} - H_{11}^s \frac{\partial^4 w_s}{\partial x^4} + F_{31}^e \frac{\partial^2 \phi}{\partial x^2} + F_{31}^m \frac{\partial^2 \gamma}{\partial x^2} - I_0 \frac{\partial^2 (w_b + w_s)}{\partial t^2} - \\ &J_1 (\frac{\partial^3 u}{\partial x \partial t^2}) + J_2 (\frac{\partial^4 w_b}{\partial x^2 \partial t^2}) + K_2 (\frac{\partial^4 w_s}{\partial x^2 \partial t^2}) - (\bar{N}) \frac{\partial^2 (w_b + w_s)}{\partial x^2} - A_{15}^e \frac{\partial^2 \phi}{\partial x^2} - A_{15}^m \frac{\partial^2 \gamma}{\partial x^2} = 0 \end{aligned} \tag{39}$$

$$A_{31}^e (\frac{\partial u}{\partial x}) - E_{31}^e \frac{\partial^2 w_b}{\partial x^2} - F_{31}^e \frac{\partial^2 w_s}{\partial x^2} + E_{15}^e \frac{\partial^2 w_s}{\partial x^2} + F_{11}^e \frac{\partial^2 \phi}{\partial x^2} + F_{11}^m \frac{\partial^2 \gamma}{\partial x^2} - F_{33}^e \phi - F_{33}^m \gamma = 0 \tag{40}$$

$$A_{31}^m (\frac{\partial u}{\partial x}) - E_{31}^m \frac{\partial^2 w_b}{\partial x^2} - F_{31}^m \frac{\partial^2 w_s}{\partial x^2} + E_{15}^m \frac{\partial^2 w_s}{\partial x^2} + F_{11}^m \frac{\partial^2 \phi}{\partial x^2} + X_{11}^m \frac{\partial^2 \gamma}{\partial x^2} - F_{33}^m \phi - X_{33}^m \gamma = 0 \tag{41}$$

3. Solution method

3.1 Analytical solution

In this section, an exact solution of the Euler-Lagrange equations for free vibration of MEE porous FG beam with simply-supported (*S*), clamped (*C*) edges or combinations of these boundary conditions is presented which they are given as (Sobhy 2013):

- Simply-supported (S)

$$w_b = w_s = N_x = M_x = 0 \qquad \text{at} \qquad x = 0, L \tag{42}$$

- Clamped (C)

$$u = w_b = w_s = \frac{\partial w_b}{\partial x} = \frac{\partial w_s}{\partial x} = 0 \qquad \text{at} \qquad x = 0, L \tag{43}$$

To satisfy above-mentioned boundary conditions, the displacement quantities are presented in the following form

$$U = \sum_{m=1}^{\infty} U_m \frac{\partial X_m(x)}{\partial x} e^{iw_m t} \tag{44}$$

$$\{W_b, W_s, \phi, \gamma\} = \sum_{m=1}^{\infty} \{W_{bm}, W_{sm}, \Phi_m, Y_m\} X_m(x) e^{iw_m t} \tag{45}$$

Where (U_m, W_{bm}, $W_{sm,}$ Φ_m, Y_m) are the unknown coefficients and the function X_m are expressed in detail in Table 2 for different boundary conditions ($\alpha = m\pi / a$). Inserting Eqs. (44)-(45) into Eqs. (37)-(41) respectively, and multiplying each equation by the corresponding displacement function then integrating over the domain of solution, leads to

$$[A_{11}r_3 + I_0\omega^2 r_1]U_m - [B_{11}r_3 + I_1\omega^2 r_1]W_b - [B_{11}^s r_3 + J_1\omega^2 r_1]W_s + [A_{31}^e r_1]\Phi_m + [A_{31}^m r_1]Y_m = 0 \tag{46}$$

$$\begin{aligned}&[B_{11}r_9 + I_1\omega^2 r_7]U_m - [D_{11}r_9 + (I_2\omega^2 + \bar{N})r_7 - I_0\omega^2 r_5]W_{bm} - \\ &[D_{11}^s r_9 + (J_2\omega^2 + \bar{N})r_7 - I_0\omega^2 r_5]W_{sm} + [E_{31}^e r_7]\Phi_m + [E_{31}^m r_7]Y_m = 0\end{aligned} \tag{47}$$

$$\begin{aligned}&[B_{11}^s r_9 + J_1\omega^2 r_7]U_m + [-D_{11}^s r_9 + I_0\omega^2 r_5 - (J_2\omega^2 + \bar{N})r_7]W_{bm} \\ &[-H_{11}^s r_9 + (A_{55}^s - \bar{N} - K_2\omega^2)r_7 + I_0\omega^2 r_5]W_{sm} + [(F_{31}^e - A_{15}^e)r_7]\Phi_m + \\ &([F_{31}^m - A_{15}^m)r_7]Y_m = 0\end{aligned} \tag{48}$$

$$A_{31}^e r_7 U_m - E_{31}^e r_7 W_{bm} + (E_{15}^e - F_{31}^e)r_7 W_{sm} + (F_{11}^e r_7 - F_{33}^e r_5)\Phi_m + (F_{11}^m r_7 - F_{33}^m r_5)Y_m = 0 \tag{49}$$

$$A_{31}^m r_7 U_m - E_{31}^m r_7 W_{bm} + (E_{15}^m - F_{31}^m)r_7 W_{sm} + (F_{11}^m r_7 - F_{33}^m r_5)\Phi_m + [X_{11}^m r_7 - X_{33}^m r_5]Y_m = 0 \tag{50}$$

where

$$(r_3, r_1) = \int_0^L (\frac{\partial^3 X_m}{\partial x^3}, \frac{\partial X_m}{\partial x}) \frac{\partial X_m}{\partial x} \tag{51}$$

$$(r_5, r_7, r_9) = \int_0^L (X_m, \frac{\partial^2 X_m}{\partial x^2}, \frac{\partial^4 X_m}{\partial x^4}) X_m \tag{52}$$

Table 2 The admissible functions $X_m(x)$ (Sobhy 2013)

Boundary conditions		The functions X_m
	At $x = 0,\ a$	$X_m(x)$
SS	$x_m(0) = x_m''(0) = x_m(a) = x_m''(a) = 0$	$\mathrm{Sin}(\alpha x)$
CS	$x_m(0) = x_m'(0) = x_m(a) = x_m''(a) = 0$	$\mathrm{Sin}(\alpha x)[\mathrm{Cos}(\alpha x) - 1]$
CC	$x_m(0) = x_m'(0) = x_m(a) = x_m'(a) = 0$	$\mathrm{Sin}^2(\alpha x)$

By finding determinant of the coefficient matrix of the following Eqs. (46)-(50) and setting this multinomial to zero, we can find natural frequencies ω_n.

4. Numerical results and discussions

In this section, numerical and graphical examples are presented to explain vibration specifications of smart MEE-FG beam with porosities based on four-variable refined beam theory. Thus, through comparisons of numerical results the impact of porosity volume fraction, FG material graduation, magnetic and electric fields, different types of porosity distributions and slenderness ratio on the natural frequency of the MEE porous FG beam will be examined. The correctness of the presented model results is compared with those of Vo *et al*. (2014) in Table 3. Hereupon $f(z)$ is considered based on higher order beam theories as $f(z) = 4z^3/3h^2$, respectively. It is indicated that the current refined beam theory and solution procedure can accurately provide non-dimensional frequency of smart porous FG beam. The non-dimensional frequency (λ) can be calculated by the relation in Eq. (53) as

$$\lambda = \omega \frac{L^2}{h}\sqrt{\frac{\rho_u}{c_{11u}}} \tag{53}$$

In Table 4, the natural frequencies of MEE-FG-(I&II) beam are elaborated to show the effect of magnetic potential for various boundary conditions (S-S, C-S and C-C) according to different values of porosity volume fractions (α = 0, 0.1, 0.2) and power-law indexes (p = 0.2, 1, 5) without electric voltage (V = 0) at (L/h = 100). Also, influence of electric voltage, porosity parameter and material graduation exponent on the natural frequency of the MEE-FG-(I&II)) beam has been detected in Table 5 for various boundary conditions (S-S, C-S and C-C). By comparing the results of these tables, it is found that negative values of magnetic potential provide lower non-dimensional frequencies of the smart FG porous beam than positive ones for all boundary conditions. But, lower values of electric voltage provide larger frequencies. This means that negative and positive values of electric voltage are cause of increment and reduction of non-dimensional frequency, respectively. Comparing the non-dimensional frequency of smart FG beam for different boundary conditions expresses that beam with stiffer edges, the stiffness of the system increases and the stiffer system produces the larger values of frequencies. Therefore, the greatest non-dimensional frequency is obtained for MEE-porous FG beam with C-C boundary condition, while the frequencies of simply supported ends (S-S) FG beam have the lowest values. Another outstanding observation is that increasing the material graduation exponents leads to reduction in the non-dimensional frequency for every type of porosity distribution. In fact, when p= 0 beam is made from fully Cobalt Ferrite ($CoFe_2O_4$) and has the greatest frequency. Increasing the material graduation exponent from 0 to 10 changes the composition of the MEE-FG beam from a fully $CoFe_2O_4$ beam to a beam with a combination of Cobalt Ferrite and barium titanate ($BaTiO_3$). So, by increasing the metal percentage and having the smaller value of Young's modulus of BaTiO3 with respect to $CoFe_2O_4$, the stiffness of system decreases. Thus, natural frequencies reduce as the stiffness of a structure decreases. In addition, it is seen that the existence of porosities has a key role on the vibration behavior of the MEE-porous FG beam, it is concluded that influence of the porosity on the vibration of MEE-FG (I) beam rely on the material graduation index (p), when the material graduation index is in the range of [0, 1], higher values of porosity volume fraction

Table 3 Comparison of non-dimensional frequency of FGM beam for different boundary condition, slenderness ratio and power-law exponents

Simply-Simply							
L/*h*		*p* = 0	*p* = 0.2	*p* = 1	*p* = 2	*p* = 5	*p* = 10
5	Vo *et al*. (2013)	5.15275	4.80590	3.97160	3.59791	3.37429	3.26534
	Present	5.15275	4.80583	3.97123	3.59852	3.37981	3.26541
20	Vo *et al*. (2013)	5.46032	5.08139	4.20387	3.83428	3.64663	3.53787
	Present	5.46032	5.08129	4.20395	3.83547	3.64892	3.53691
Clamped-Clamped							
L/*h*		*p* = 0	*p* = 0.2	*p* = 1	*p* = 2	*p* = 5	*p* = 10
5	Vo *et al*. (2013)	10.06780	9.46237	7.95221	7.18011	6.49614	6.16623
	Present	10.06780	9.46259	7.95571	7.18942	6.49867	6.16541
20	Vo *et al*. (2013)	12.22280	11.38380	9.43282	8.59942	8.14595	7.88616
	Present	12.22280	11.38561	9.43653	8.59831	8.14713	7.88722

Table 4 Effect of porosity volume fraction and magnetic potential on the non-dimensional frequency of MEE-FG beam under different boundary conditions (*L*/*h* = 100, *V* = 0)

Even porosity							
B.C	Ω	α = 0			α = 0.2		
		p = 0.2	*p* = 1	*p* = 5	*p* = 0.2	*p* = 1	*p* = 5
S-S	-500	0.71065	1.18126	1.66022	0.620912	1.22405	1.82798
	0	2.16524	2.02602	1.92318	2.19704	2.02006	1.89108
	500	2.97581	2.61039	2.15428	3.04441	2.58127	1.95214
C-S	-500	3.48039	3.48987	3.66327	3.49732	3.50292	3.74895
	0	4.33659	4.06374	3.86357	4.39741	4.04393	3.79865
	500	5.04695	4.56605	4.05398	5.14229	4.53138	3.84779
C-C	-500	4.41544	4.28853	4.31745	4.45636	4.29005	4.34958
	0	5.00736	4.69083	4.46057	5.0775	4.67413	4.38540
	500	5.53635	5.06125	4.59925	5.63052	5.02896	4.42092
Uneven porosity							
B.C	Ω	α = 0			α = 0.2		
		p = 0.2	*p* = 1	*p* = 5	*p* = 0.2	*p* = 1	*p* = 5
S-S	-500	0.71065	1.18126	1.66022	0.830708	1.28622	1.80067
	0	2.16524	2.02602	1.92318	2.23345	2.08008	1.96711
	500	2.97581	2.61039	2.15428	3.04738	2.64558	2.12053
C-S	-500	3.48039	3.48987	3.66327	3.62313	3.62324	3.82263
	0	4.33659	4.06374	3.86357	4.47258	4.171174	3.95169
	500	5.04695	4.56605	4.05398	5.18466	4.65607	4.07666
C-C	-500	4.41544	4.28853	4.31745	4.57601	4.42984	4.46966
	0	5.00736	4.69083	4.46057	5.16436	4.81524	4.56223
	500	5.53635	5.06125	4.59925	5.69222	5.17200	4.65297

Table 5 Effect of porosity volume fraction and electric voltage on the non-dimensional frequency of MEE-FG beam under different boundary conditions (L/h = 100, Ω = 0)

Even porosity							
B.C	V	α = 0			α = 0.2		
		p = 0.2	p = 1	p = 5	p = 0.2	p = 1	p = 5
S-S	-500	2.18554	2.08431	2.01591	2.20692	2.07716	1.98979
	0	2.16524	2.02602	1.92318	2.19704	2.02206	1.89108
	500	2.14476	1.96601	1.82575	2.18712	1.96130	1.78962
C-S	-500	4.35285	4.11063	3.93847	4.40532	4.09588	3.87852
	0	4.33659	4.06374	3.86357	4.39741	4.04393	3.79865
	500	4.32027	4.0163	3.78718	4.38949	4.00345	3.71714
C-C	-500	5.01910	4.72475	4.51484	5.0832	4.70738	4.44325
	0	5.00736	4.69083	4.46057	5.0775	4.67413	4.38540
	500	4.99559	4.65665	4.40565	5.07178	4.64064	4.32677
Uneven porosity							
B.C	V	α = 0			α = 0.2		
		p = 0.2	p = 1	p = 5	p = 0.2	p = 1	p = 5
S-S	-500	2.18554	2.08431	2.01591	2.21873	2.13651	2.0598
	0	2.16524	2.02602	1.92318	2.23345	2.08008	1.96711
	500	2.14476	1.96601	1.82575	2.21806	2.02207	1.86984
C-S	-500	4.35285	4.11063	3.93847	4.48481	4.21712	4.02654
	0	4.33659	4.06374	3.86357	4.47258	4.17117	3.95169
	500	4.32027	4.0163	3.78718	4.4603	4.12586	3.8754
C-C	-500	5.01910	4.72475	4.51484	5.1732	4.84807	4.61645
	0	5.00736	4.69083	4.46057	5.16436	4.81524	4.56223
	500	4.99559	4.65665	4.40565	5.15551	4.78218	4.50736

provide larger values of the frequency results while this trend is vice versa by increasing of power-law index. But for MEE-FG (II) beam, higher values of porosity volume fraction provide larger values of the frequency results for all material graduation index. Comparing results of even and uneven porosity distributions reveals that the porosity has more significant impact on natural frequencies of the MEE-FG (I) than MEE-FG (II) at every magnetic potentials and electric voltages.

To indicate the effect of porosity on the vibration response of MEE-FG beam, Fig. 2 depicts variations of the first non-dimensional natural frequency of S-S MEE-FGM-I &-II beam with material graduation and porosity parameter at a constant value of slenderness ratio (L/h = 100), magnetic potential (Ω = 0) and electric voltage (V = 0). It is clear from the curve that porosity effect according to the even distribution relies on the value of power-law index. For example, by increasing the porosity parameter the natural frequency first increases at lower gradient indexes, however, an opposite behavior is observed from a certain value of the power index. In other words, from a certain value of power-law index, increasing porosity volume fraction leads to lower non-dimensional frequencies. It means that, for MEE-FGM model with even porosity distribution when the power-law exponent is approximately lower than 2, the frequency increases due to increasing

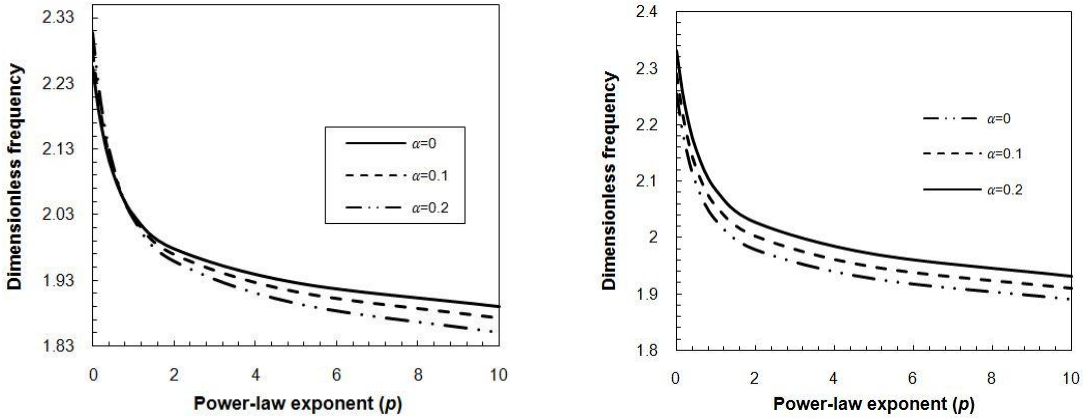

(a) Even porosity (b) Uneven porosity

Fig. 2 The variation of the first dimensionless frequency of S-S MEE-FGM porous beam with material graduation and porosity parameter (L/h = 20, Ω = 0, V = 0)

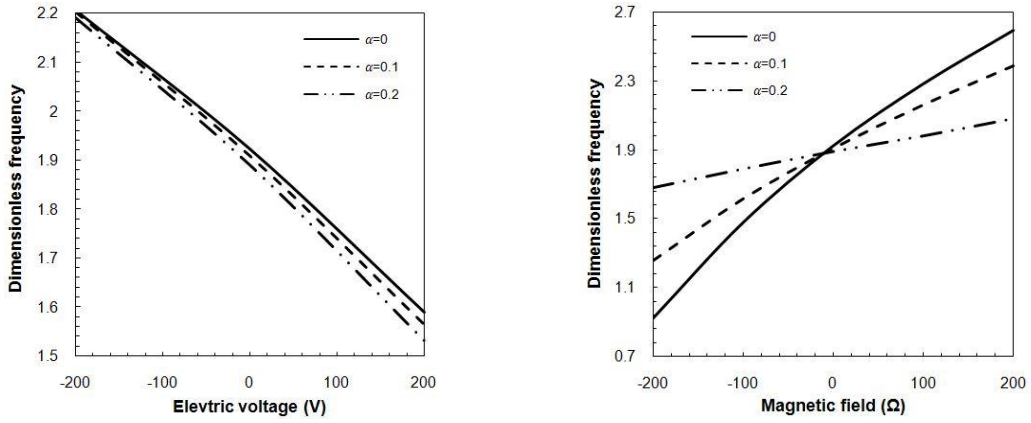

Ω = 0 α = 0.2, Ω = 0

Fig. 3 Effect of porosity volume index on the dimensionless frequency of the S-S MEE-FGM (I) beam with respect to applied magnetics potential and electric voltage (L/h = 100, p = 5)

of the porosity parameter, while for higher values of gradient indexes the frequencies decrease by increasing the porosities. Moreover, it is observed that non-dimensional frequency of MEE-FG plates with uneven porosity distribution increases as the porosity parameter increases for every value of power-law exponent. In other words, the decreasing nature of the curve shows the moderate values of non-dimensional frequency taken by 0.1 porosity parameter, highest value taken by 0.2 porosity volume fraction and lowest values taken by perfect FGM (α = 0). Hence, it can be concluded that vibration behavior of MEE-porous FG beam is affected by the type of porosity distribution. Beside this, it is seen that increasing the material graduation index is cause of reduction in non-dimensional frequency results of the MEE-FG porous beam. This is due to this fact that, increasing the power-law exponent leads to decrease in the bending rigidity and elasticity modulus and as also known from the theory of vibrations, the natural frequencies are directly proportional with the rigidity and elasticity modulus.

The variations of natural frequency of the simply-supported smart MEE-FG (I) beam subjected to external magnetic potential and electric voltage for different values of porosity volume fractions at (L/h = 100, p = 5) are presented in Fig. 3, respectively. It is found that external electric voltage and magnetic potential respectively indicates reducing and increasing impacts on the frequency of MEE porous beam when their values varies from negative to positive one at a fixed value of porosity volume fraction which highlights the notability of the sign of magnetic potential and electric voltage. Furthermore, according to these tables the non-dimensional frequency decreases as the porosity value increases for all values of electric voltage but it depends on the sign and magnitude of magnetic potential.

In order to peruse the effect of magnetic field and electric voltage on the natural frequencies of the smart S-S MEE-FGM beam, the natural frequency variation, versus the slenderness ratio for perfect FGM and imperfect FGM (α = 0.2) at constant value of material graduation (p = 5), is plotted in Fig. 4. One may deduce that when external electric voltage and magnetic potential are zero, dimensionless frequency is not dependent on the slenderness ratio. Also, it is observable that higher values of a/h have more significant influence on frequency response. Moreover, it can be

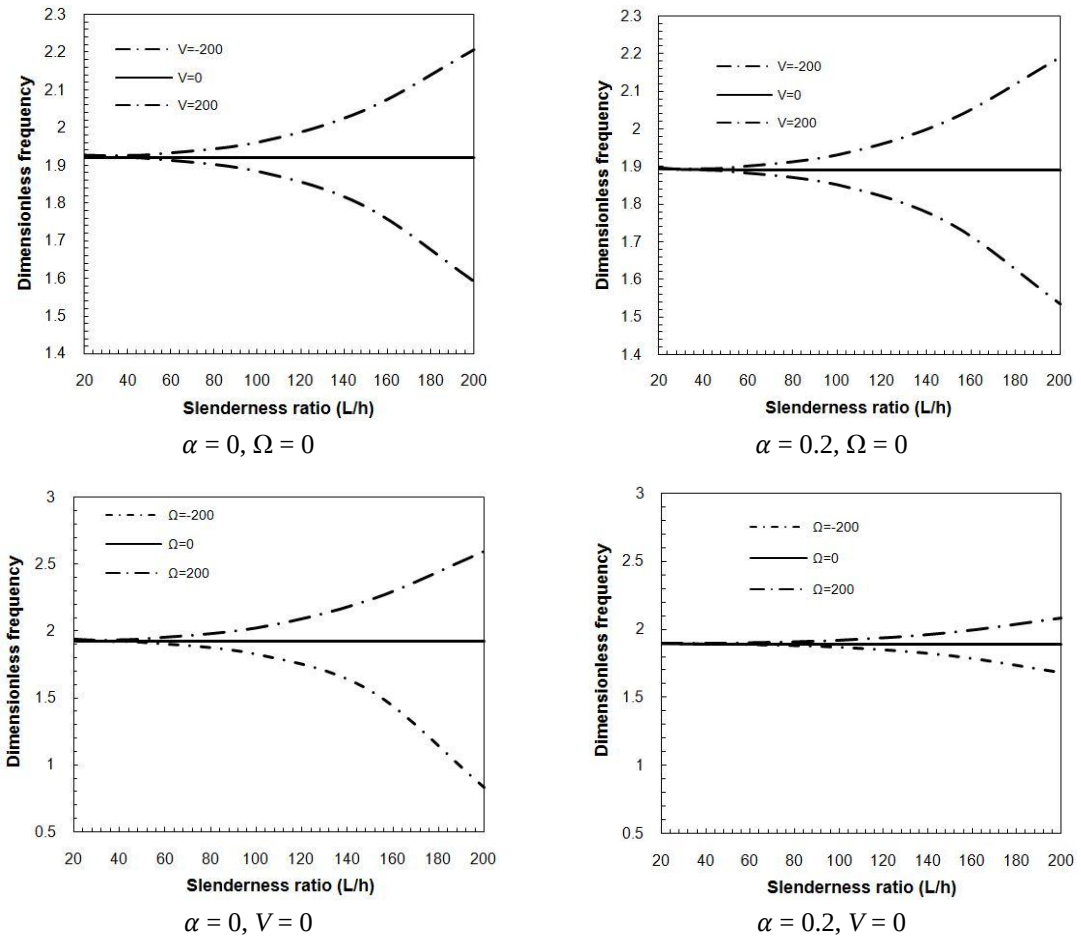

Fig. 4 Effect of slenderness ratio on the dimensionless frequency of S-S MEE-FGM(I) beam for various magnetic potentials and electric voltages (p = 5)

seen that exerting negative voltages lead to higher frequencies, but exerting negative magnetic potentials lead to lower frequencies. Consequently, the difference between frequency results according to negative and positive values of electric and magnetic fields increases with the rise of side-to-thickness ratio. So, it is concluded that influence of electric voltage and magnetic potential is more obvious in higher values of L/h.

Fig. 5 demonstrates the influence of different boundary conditions on the non-dimensional frequency of MEE-FG beam with respect to even and uneven porosity distributions, respectively at L/h = 100, V = 200, Ω = 100 and p = 5. It is clear that natural frequency recorded for Simply-Simply boundary condition takes the lowest value, while it is medium for Clamped-Simply boundary condition. However, the value of natural frequency shoots up for the Clamped-Clamped boundary condition. It can also be noted that, influence of porosity parameter on the natural frequency of MEE-FG beam with even and uneven porosity distributions is similar previous

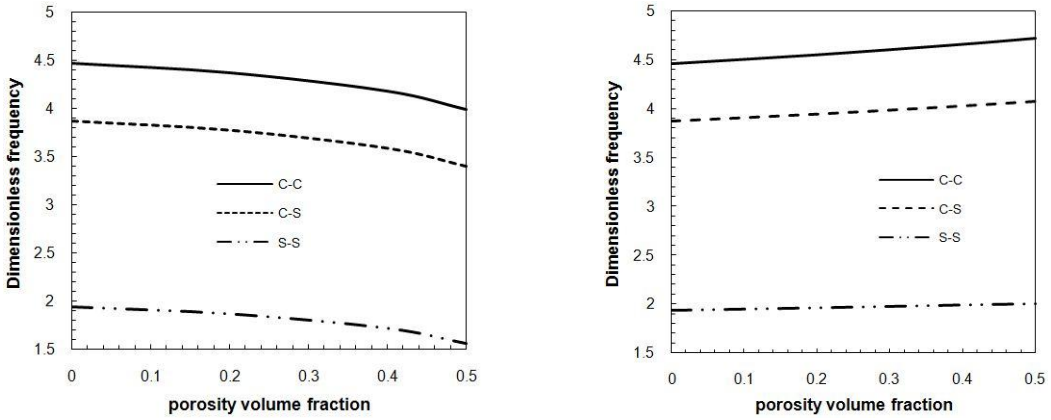

(a) Even porosity (b) Uneven porosity

Fig. 5 Effect of porosity volume index on the dimensionless frequency of MEE-FGM (I&II) beam with different boundary condition (L/h = 100, V = 200, Ω = 100, p = 5)

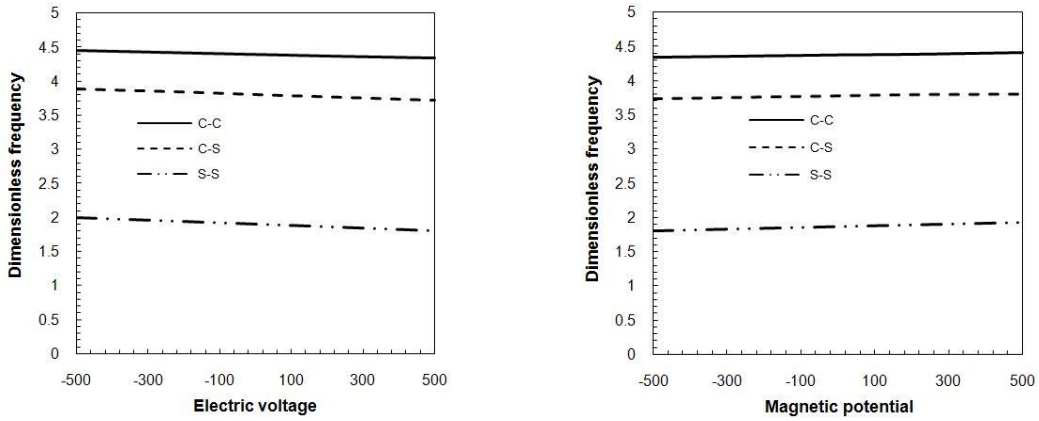

Ω = 100 V = 100

Fig. 6 Effect of electric voltage and magnetic potential on the dimensionless frequency of different boundary FGM (I) beam (L/h = 100, p = 5, α = 0.2)

conclusions for all boundary conditions. Hence, even and uneven porosity respectively provide lower and higher natural frequencies for MEE-FG beam at $p = 5$.

The natural frequency of smart porous FG beam associated with electric voltage and magnetic potential for different boundary conditions at $L/h = 100$, $p = 5$ and $\alpha = 0.2$ are shown respectively in Fig. 6. It is pointed out that for all types of boundary conditions increasing the external voltage causes reduction of the natural frequency while increasing the magnetic potential results in increasing non-dimensional frequency. Thus, magnitude and sign of electric and magnetic fields have significant role on vibration behavior of porous MEE-FG beam.

5. Conclusions

In the proposed investigation, vibration characteristics of smart functionally graded (MEE-FG) beam with porosities subjected to magnet electro fields under different boundary conditions is implemented within the framework of a four-variable higher order shear deformation theory in which verify shear deformation effect regardless of any shear correction factor. The influence of different types of porosity distributions namely even and uneven distributions and various boundary conditions on vibrational responses of MEE-porous FG beams are considered. Mechanical properties of the smart porous MEE-FG beam vary in the thickness direction based on modified power-law model for approximation of material properties with even and uneven distributions of porosities. The governing differential equations of motion and boundary conditions are derived by using Hamilton principle and then solved by applying an analytical solution method for various boundary conditions. Accuracy of the results is examined using available date in the literature. It is indicated that the vibration characteristics of MEE- porous FGM beam are significantly affected by various parameters such as slenderness ratio, magnetic field, external electric voltage, volume fraction of porosity, material graduation, various boundary conditions and porosity distribution. Numerical results show that:

- As growing the power-law exponent, natural frequencies of porous MEE-FG beam are found to diminish.
- For MEE-porous FGM beam with even porosity distribution, increasing the volume fraction of porosity first is cause of increment in non-dimensional frequency, then this trend becomes opposite for higher values of material graduation index.
- Non-dimensional frequency of MEE-porous FG beam with uneven porosity distribution increases with increment in porosity parameters for all values of material graduation index.
- Increasing magnetic potential yields increment of non-dimensional frequency of porous MEE-FGM beam. However, for the external electric voltage this behavior is opposite.
- Effect of porosity volume fraction on natural frequency rely on porosity distribution and power-law index.
- The non-dimensional frequency of MEE- porous FGM beam with C-C boundary condition is greatest, followed by C-S and S-S respectively.
- Effect of slenderness ratio (L/h) on frequencies with respect to magnetic potentials and electric voltages is more prominent at its higher values. As slenderness ratio increases, the difference between frequency results according to negative and positive values of magnetic fields and electric voltage increases and this difference is more noticeable for perfect MEE-FG beam.

References

Akbas, S.D. (2015), "Wave propagation of a functionally graded beam in thermal environments", *Steel Compos. Struct., Int. J.*, **19**(6), 1421-1447.

Benferhat, R., Hassaine, D., Hadji, L. and Said, M. (2016), "Static analysis of the FGM plate with porosities", *Steel Compos. Struct., Int. J.*, **21**(1), 123-136.

Chen, W., Lee, K.Y. and Ding, H. (2005), "On free vibration of non-homogeneous transversely isotropic magneto-electro-elastic plates", *J. Sound Vib.*, **279**(1), 237-251.

Daga, A., Ganesan, N. and Shankar, K. (2009), "Transient dynamic response of cantilever magneto-electro-elastic beam using finite elements", *Int. J. Comput. Method. Eng. Sci. Mech.*, **10**(3), 173-185.

Ebrahimi, F. (2013), "Analytical investigation on vibrations and dynamic response of functionally graded plate integrated with piezoelectric layers in thermal environment", *Mech. Adv. Mater. Struct.*, **20**(10), 854-870.

Ebrahimi, F. and Barati, M.R. (2016a), "A nonlocal higher-order shear deformation beam theory for vibration analysis of size-dependent functionally graded nanobeams", *Arab. J. Sci. Eng.*, **41**(5), 1679-1690.

Ebrahimi, F. and Barati, M.R. (2016b), "Vibration analysis of nonlocal beams made of functionally graded material in thermal environment", *Eur. Phys. J. Plus*, **131**(8), 279.

Ebrahimi, F. and Barati, M.R. (2016c), "Buckling analysis of smart size-dependent higher order magneto-electro-thermo-elastic functionally graded nanosize beams", *J. Mech.*, 1-11.

Ebrahimi, F. and Barati, M.R. (2016d), "On nonlocal characteristics of curved inhomogeneous Euler–Bernoulli nanobeams under different temperature distributions", *Appl. Phys. A*, **122**(10), 880.

Ebrahimi, F. and Barati, M.R. (2016e), "A nonlocal higher-order refined magneto-electro-viscoelastic beam model for dynamic analysis of smart nanostructures", *Int. J. Eng. Sci.*, **107**, 183-196.

Ebrahimi, F. and Barati, M.R. (2016f), "Hygrothermal effects on vibration characteristics of viscoelastic FG nanobeams based on nonlocal strain gradient theory", *Compos. Struct.*, **159**, 433-444.

Ebrahimi, F. and Barati, M.R. (2016g), "Buckling analysis of nonlocal third-order shear deformable functionally graded piezoelectric nanobeams embedded in elastic medium", *J. Brazil. Soc. Mech. Sci. Eng.*, 1-16.

Ebrahimi, F. and Barati, M.R. (2016h), "Magnetic field effects on buckling behavior of smart size-dependent graded nanoscale beams", *Eur. Phys. J. Plus*, **131**(7), 1-14.

Ebrahimi, F. and Barati, M.R. (2016i), "Buckling analysis of smart size-dependent higher order magneto-electro-thermo-elastic functionally graded nanosize beams", *J. Mech.*, 1-11.

Ebrahimi, F. and Barati, M.R. (2016j), "Flexural wave propagation analysis of embedded S-FGM nanobeams under longitudinal magnetic field based on nonlocal strain gradient theory", *Arab. J. Sci. Eng.*, 1-12.

Ebrahimi, F. and Barati, M.R. (2016k), "Wave propagation analysis of quasi-3D FG nanobeams in thermal environment based on nonlocal strain gradient theory", *Appl. Phys. A*, **122**(9), 843.

Ebrahimi, F. and Barati, M.R. (2016l), "An exact solution for buckling analysis of embedded piezoelectro-magnetically actuated nanoscale beams", *Adv. Nano Res., Int. J.*, **4**(2), 65-84.

Ebrahimi, F. and Barati, M.R. (2016m), "Electromechanical buckling behavior of smart piezoelectrically actuated higher-order size-dependent graded nanoscale beams in thermal environment", *Int. J. Smart Nano Mater.*, **7**(2), 69-90.

Ebrahimi, F. and Barati, M.R. (2016n), "Small scale effects on hygro-thermo-mechanical vibration of temperature dependent nonhomogeneous nanoscale beams", *Mech. Adv. Mater. Struct.*, 1-13.

Ebrahimi, F. and Barati, M.R. (2016o), "Temperature distribution effects on buckling behavior of smart heterogeneous nanosize plates based on nonlocal four-variable refined plate theory", *Int. J. Smart Nano Mater.*, **7**(3), 1-25.

Ebrahimi, F. and Barati, M.R. (2016p), "Buckling analysis of piezoelectrically actuated smart nanoscale plates subjected to magnetic field", *J. Intel. Mater. Syst. Struct.*, 1045389X16672569.

Ebrahimi, F. and Barati, M.R. (2016q), "Thermal environment effects on wave dispersion behavior of

inhomogeneous strain gradient nanobeams based on higher order refined beam theory", *J. Therm. Stress.*, **39**(12), 1560-1571.
Ebrahimi, F. and Barati, M.R. (2016r), "Vibration analysis of nonlocal beams made of functionally graded material in thermal environment", *Eur. Phys. J. Plus*, **131**(8), 279.
Ebrahimi, F. and Barati, M.R. (2016s), "A unified formulation for dynamic analysis of nonlocal heterogeneous nanobeams in hygro-thermal environment", *Appl. Phys. A*, **122**(9), 792.
Ebrahimi, F. and Barati, M.R. (2017), "A nonlocal strain gradient refined beam model for buckling analysis of size-dependent shear-deformable curved FG nanobeams", *Compos. Struct.*, **159**, 174-182.
Ebrahimi, F. and Boreiry, M. (2015), "Investigating various surface effects on nonlocal vibrational behavior of nanobeams", *Appl. Phys. A*, **121**(3), 1305-1316.
Ebrahimi, F. and Hosseini, S.H.S. (2016a), "Thermal effects on nonlinear vibration behavior of viscoelastic nanosize plates", *J. Therm. Stress.*, **39**(5), 606-625.
Ebrahimi, F. and Hosseini, S.H.S. (2016b), "Nonlinear electroelastic vibration analysis of NEMS consisting of double-viscoelastic nanoplates", *Appl. Phys. A*, **122**(10), 922.
Ebrahimi, F. and Hosseini, S.H.S. (2016c), "Double nanoplate-based NEMS under hydrostatic and electrostatic actuations", *Eur. Phys. J. Plus*, **131**(5), 1-19.
Ebrahimi, F. and Jafari, A. (2016a), "Thermo-mechanical vibration analysis of temperature-dependent porous FG beams based on Timoshenko beam theory", *Struct. Eng. Mech., Int. J.*, **59**(2), 343-371.
Ebrahimi, F. and Jafari, A. (2016b), "A higher-order thermomechanical vibration analysis of temperature-dependent FGM beams with porosities", *J. Eng.*
Ebrahimi, F. and Mokhtari, M. (2014), "Transverse vibration analysis of rotating porous beam with functionally graded microstructure using the differential transform method", *J. Brazil. Soc. Mech. Sci. Eng.*, **37**(4), 1435-1444.
Ebrahimi, F. and Rastgoo, A. (2009), "Nonlinear vibration of smart circular functionally graded plates coupled with piezoelectric layers", *Int. J. Mech. Mater. Des.*, **5**(2), 157-165.
Ebrahimi, F. and Rastgoo, A. (2011), "Nonlinear vibration analysis of piezo-thermo-electrically actuated functionally graded circular plates", *Archive Appl. Mech.*, **81**(3), 361-383.
Ebrahimi, F. and Salari, E (2015a), "Nonlocal thermo-mechanical vibration analysis of functionally graded nanobeams in thermal environment", *Acta Astronautica*, **113**, 29-50.
Ebrahimi, F. and Salari, E. (2015b), "Size-dependent thermo-electrical buckling analysis of functionally graded piezoelectric nanobeams", *Smart Mater. Struct.*, **24**(12), 125007.
Ebrahimi, F. and Salari, E. (2015c), "Thermo-mechanical vibration analysis of a single-walled carbon nanotube embedded in an elastic medium based on higher-order shear deformation beam theory", *J. Mech. Sci. Technol.*, **29**(9), 3797-3803.
Ebrahimi, F. and Salari, E. (2015d), "Size-dependent thermo-electrical buckling analysis of functionally graded piezoelectric nanobeams", *Smart Mater. Struct.*, **24**(12), 125007.
Ebrahimi, F. and Salari, E. (2016), "Effect of various thermal loadings on buckling and vibrational characteristics of nonlocal temperature-dependent functionally graded nanobeams", *Mech. Adv. Mater. Struct.*, **23**(12), 1379-1397.
Ebrahimi, F. and Sepiani, H. (2010), "Transverse shear and rotary inertia effects on the stability analysis of functionally graded shells under combined static and periodic axial loadings", *J. Mech. Sci. Technol.*, **24**(12), 2359-2366.
Ebrahimi, F. and Shafiei, N. (2016), "Influence of initial shear stress on the vibration behavior of single-layered graphene sheets embedded in an elastic medium based on Reddy's higher-order shear deformation plate theory", *Mech. Adv. Mater. Struct.*, 1-41.
Ebrahimi, F. and Zia, M. (2015), "Large amplitude nonlinear vibration analysis of functionally graded Timoshenko beams with porosities", *Acta Astronautica*, **116**, 117-125.
Ebrahimi, F., Naei, M.H. and Rastgoo, A. (2009), "Geometrically nonlinear vibration analysis of piezoelectrically actuated FGM plate with an initial large deformation", *J. Mech. Sci. Technol.*, **23**(8), 2107-2124.
Ebrahimi, F., Rastgoo, A. and Bahrami, M.N. (2010), "Investigating the thermal environment effects on

geometrically nonlinear vibration of smart functionally graded plates", *J. Mech. Sci. Technol.*, **24**(3), 775-791.
Ebrahimi, F., Ghadiri, M., Salari, E., Hoseini, S.A.H. and Shaghaghi, G.R. (2015a), "Application of the differential transformation method for nonlocal vibration analysis of functionally graded nanobeams", *J. Mech. Sci. Technol.*, **29**(3), 1207-1215.
Ebrahimi, F., Salari, E. and Hosseini, S.A.H. (2015b), "Thermomechanical vibration behavior of FG nanobeams subjected to linear and nonlinear temperature distributions", *J. Therm. Stress.*, **38**(12), 1360-1386.
Ebrahimi, F., Barati, M.R. and Dabbagh, A. (2016a), "Wave dispersion characteristics of axially loaded magneto-electro-elastic nanobeams", *Appl. Phys. A*, **122**(11), 949.
Ebrahimi, F., Barati, M.R. and Dabbagh, A. (2016b), "A nonlocal strain gradient theory for wave propagation analysis in temperature-dependent inhomogeneous nanoplates", *Int. J. Eng. Sci.*, **107**, 169-182.
Ebrahimi, F., Barati, M.R. and Haghi, P. (2016c), "Nonlocal thermo-elastic wave propagation in temperature-dependent embedded small-scaled nonhomogeneous beams", *Eur. Phys. J. Plus*, **131**(11), 383.
Ebrahimi, F., Barati, M.R. and Haghi, P. (2016d), "Thermal effects on wave propagation characteristics of rotating strain gradient temperature-dependent functionally graded nanoscale beams", *J. Therm. Stress.*, 1-13.
Ebrahimi, F., Salari, E. and Hosseini, S.A.H. (2016e), "In-plane thermal loading effects on vibrational characteristics of functionally graded nanobeams", *Meccanica*, **51**(4), 951-977.
Ebrahimi, F., Ghasemi, F. and Salari, E. (2016f), "Investigating thermal effects on vibration behavior of temperature-dependent compositionally graded Euler beams with porosities", *Meccanica*, **51**(1), 223-249.
Harshe, G., Dougherty, J. and Newnham, R. (1993), "Theoretical modelling of multilayer magnetoelectric composites", *Int. J. Appl. Electromagnet. Mater.*, **4**(2), 145-145.
Huang, D., Ding, H. and Chen, W. (2007), "Analytical solution for functionally graded magneto-electro-elastic plane beams", *Int. J. Eng. Sci.*, **45**(2), 467-485.
Jiang, A. and Ding, H. (2004), "Analytical solutions to magneto-electro-elastic beams", *Struct. Eng. Mech., Int. J.*, **18**(2), 195-209.
Kattimani, S. and Ray, M. (2015), "Control of geometrically nonlinear vibrations of functionally graded magneto-electro-elastic plates", *Int. J. Mech. Sci.*, **99**, 154-167.
Ke, L.-L. and Wang, Y.-S. (2014), "Free vibration of size-dependent magneto-electro-elastic nanobeams based on the nonlocal theory", *Physica E: Low-Dimens. Syst. Nanostruct.*, **63**, 52-61.
Kumaravel, A., Ganesan, N. and Sethuraman, R. (2007), "Buckling and vibration analysis of layered and multiphase magneto-electro-elastic beam under thermal environment", *Multidiscipl. Model. Mater. Struct.*, **3**(4), 461-476.
Lang, Z. and Xuewu, L. (2013), "Buckling and vibration analysis of functionally graded magneto-electro-thermo-elastic circular cylindrical shells", *Appl. Math. Model.*, **37**(4), 2279-2292.
Mantari, J., Bonilla, E. and Soares, C.G. (2014), "A new tangential-exponential higher order shear deformation theory for advanced composite plates", *Compos. Part B: Eng.*, **60**, 319-328.
Mechab, I., Mechab, B., Benaissa, S., Serier, B. and Bouiadjra, B.B. (2016), "Free vibration analysis of FGM nanoplate with porosities resting on Winkler Pasternak elastic foundations based on two-variable refined plate theories", *J. Brazil. Soc. Mech. Sci. Eng.*, **38**(8), 2193-2211.
Pan, E. (2001), "Exact solution for simply supported and multilayered magneto-electro-elastic plates", *J. Appl. Mech.*, **68**(4), 608-618.
Pan, E. and Han, F. (2005), "Exact solution for functionally graded and layered magneto-electro-elastic plates", *Int. J. Eng. Sci.*, **43**(3), 321-339.
Rezaei, A. and Saidi, A. (2016), "Application of Carrera Unified Formulation to study the effect of porosity on natural frequencies of thick porous–cellular plates", *Compos. Part B: Eng.*, **91**, 361-370.
Razavi, S. and Shooshtari, A. (2015), "Nonlinear free vibration of magneto-electro-elastic rectangular plates", *Compos. Struct.*, **119**, 377-384.

Sladek, J., Sladek, V., Krahulec, S., Chen, C. and Young, D. (2015), "Analyses of Circular Magnetoelectroelastic Plates with Functionally Graded Material Properties", *Mech. Adv. Mater. Struct.*, **22**(6), 479-489.

Sobhy, M. (2013), "Buckling and free vibration of exponentially graded sandwich plates resting on elastic foundations under various boundary conditions", *Compos. Struct.*, **99**, 76-87.

Song, G., Sethi, V. and Li, H.-N. (2006), "Vibration control of civil structures using piezoceramic smart materials: a review", *Eng. Struct.*, **28**(11), 1513-1524.

Wattanasakulpong, N. and Chaikittiratana, A. (2015), "Flexural vibration of imperfect functionally graded beams based on Timoshenko beam theory: Chebyshev collocation method", *Meccanica*, **50**(5), 1331-1342.

Wattanasakulpong, N. and Ungbhakorn, V. (2014), "Linear and nonlinear vibration analysis of elastically restrained ends FGM beams with porosities", *Aerosp. Sci. Technol.*, **32**(1), 111-120.

Wattanasakulpong, N., Prusty, B.G., Kelly, D.W. and Hoffman, M. (2012), "Free vibration analysis of layered functionally graded beams with experimental validation", *Mater. Des.*, **36**, 182-190.

Wu, C.-P. and Tsai, Y.-H. (2007), "Static behavior of functionally graded magneto-electro-elastic shells under electric displacement and magnetic flux", *Int. J. Eng. Sci.*, **45**(9), 744-769.

Wu, C.-P. and Tsai, Y.-H. (2010), "Dynamic responses of functionally graded magneto-electro-elastic shells with closed-circuit surface conditions using the method of multiple scales", *Eur. J. Mech.-A/Solids*, **29**(2), 166-181.

Wu, C.-P., Chen, S.-J. and Chiu, K.-H. (2010), "Three-dimensional static behavior of functionally graded magneto-electro-elastic plates using the modified Pagano method", *Mech. Res. Commun.*, **37**(1), 54-60.

Xin, L. and Hu, Z. (2015), "Free vibration of layered magneto-electro-elastic beams by SS-DSC approach", *Compos. Struct.*, **125**, 96-103.

Yahia, S.A., Atmane, H.A., Houari, M.S.A. and Tounsi, A. (2015), "Wave propagation in functionally graded plates with porosities using various higher-order shear deformation plate theories", *Struct. Eng Mech., Int. J.*, **53**(6), 1143-1165.

Zhang, R., Duan, Y., Or, S.W. and Zhao, Y. (2014), "Smart elasto-magneto-electric (EME) sensors for stress monitoring of steel cables: design theory and experimental validation", *Sensors*, **14**(8), 13644-13660.

Zhu, J., Lai, Z., Yin, Z., Jeon, J. and Lee, S. (2001), "Fabrication of ZrO 2–NiCr functionally graded material by powder metallurgy", *Mater. Chem. Phys.*, **68**(1), 130-135.

JL